ACS APPLIED BIO MATERIALS

www.acsabm.org Article

Poly-L-lysine/Laminin Surface Coating Reverses Glial Cell Mechanosensitivity on Stiffness-Patterned Hydrogels

Caterina Tomba,* Camille Migdal, David Fuard, Catherine Villard, and Alice Nicolas*

Cite This: https://doi.org/10.1021/acsabm.1c01295 Read Online

ACCESS | Metrics & More | Article Recommendations | Supporting Information

ABSTRACT: Brain tissues demonstrate heterogeneous mechanical properties, which evolve with aging and pathologies. The observation in these tissues of smooth to sharp rigidity gradients raises the question of brain cell responses to both different values of rigidity and their spatial variations, in dependence on the surface chemistry they are exposed to. Here, we used recent techniques of hydrogel photopolymerization to achieve stiffness texturing down to micrometer resolution in polyacrylamide hydrogels. We investigated primary neuron adhesion and orientation as well as glial cell proliferative properties on these rigidity-textured hydrogels for two adhesive coatings: fibronectin or poly-L-lysine/laminin. Our main observation is that glial cell adhesion and proliferation is favored on the stiffer regions when the adhesive coating is fibronectin and on the softer ones when it consists of poly-L-lysine/laminin. This behavior was unchanged by the presence or the absence of neuronal cells. In addition, glial cells were not confined by sharp, micron-scaled gradients of rigidity. Our observations suggest that rigidity sensing could involve adhesion-related pathways that profoundly depend on surface chemistry.

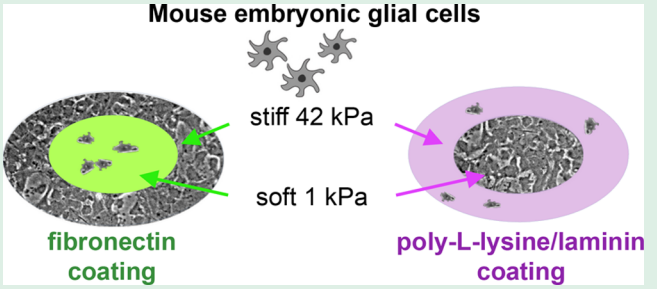

KEYWORDS: *polyacrylamide hydrogels, stiffness patterns, surface functionalization, mechanosensitivity, primary brain cells*

1. INTRODUCTION

The mechanical properties of the extracellular matrix (ECM) have been shown for long to induce significant changes on the cell structure and functions in many cell types like fibroblasts or HeLa cells[1] or even stem cells including neural stem cells.[2] For the last two decades, both in vitro[3−5] and in vivo[6,7] studies have been conducted. Mechanical cues were for example shown to drive the epithelial to mesenchymal transition in vitro,[8] and a recent in vivo study demonstrated that tumor propagation can be mediated by mechanical signaling pathways.[9] Concerning brain cells, in vitro studies showed that neurons are sensitive to the rigidity of the ECM. Neurites have been reported to extend longer extensions on soft matrices, below 1 kPa, compared to stiffer substrates, either in 2D and in 3D.[10−17] Consequently, the mechanosensitivity of the growth cone has been investigated.[12,14,17−20] Neuron rigidity sensing was shown to be integrin-dependent,[14] and the growth of axons was shown to be directed toward the softest part of the matrix.[21] Links between the mechanical properties of the brain tissues, which are built from as many neurons as glial cells, and brain functions were also evidenced in vivo.[22]

Glial cells however have received less attention, although their active and specific functions in brain computation[23] as well as their multiple roles beyond providing cohesion of the brain tissue (glia coming from the Greek for "glue") are increasingly understood.[24] For instance, astrocytes, a subtype of glial cells, are involved in the response to traumatic brain insults[25,26] and in cancers[27] from their intrinsic ability to proliferate and secrete tumorigenic factors. It is therefore crucial to better understand their response to the different stimuli (chemical, topographical, mechanical) provided by their microenvironments. At the cell level, these cues trigger various cellular adaptations concerning adhesion, polarization, migration, or proliferation among others.[28,29] Astrocytes were also shown to be sensitive to rigidity, but unlike neurons, they were reported to display better adhesion and a larger spreading area on stiff substrates rather than on soft ones when cultured on laminin or poly-D-lysine coatings.[11,25,26,30]

In the present work, we address the influence of the mechanical heterogeneities of the ECM on primary brain cell sensitivity to rigidity in vitro, in dependence with surface chemistry, cell seeding composition, and culture medium. To this end, we analyzed the initial adhesion, growth, and proliferation of primary neurons and glial cells (i.e., mostly astrocytes) dissociated from the mouse embryo cortex and hippocampal tissues on ECM with nonuniform mechanical properties but a uniform coating of adhesive ligands. More

Received: December 22, 2021
Accepted: March 1, 2022

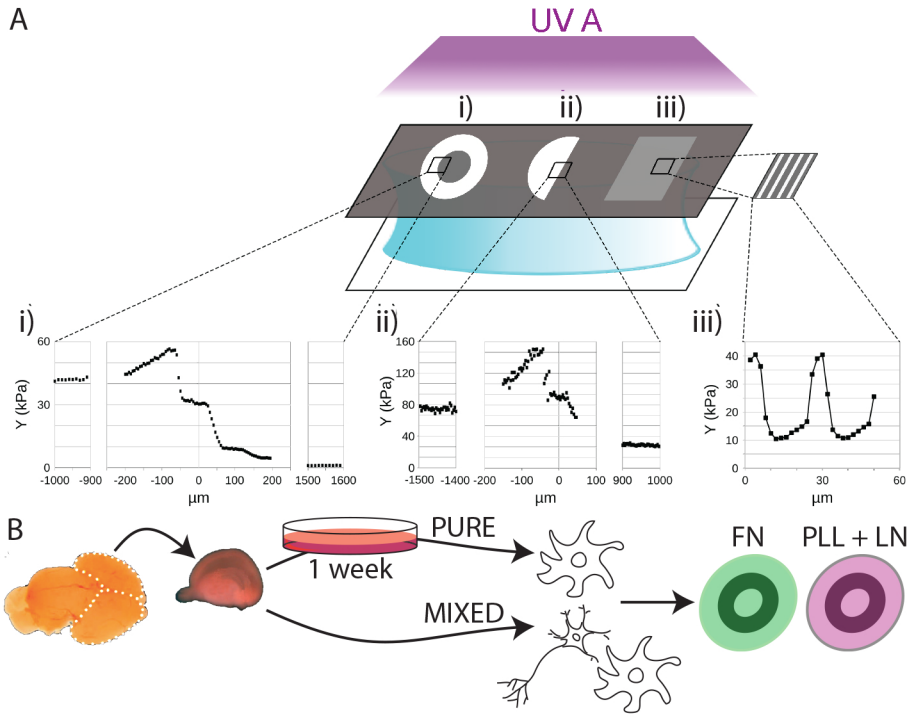

Figure 1. Technology for the fabrication of the culture supports and design of the experiment. (A) The rigidity patterns are obtained by photopolymerization of polyacrylamide hydrogels through gray leveled masks: (i) "Concentric" design, millimeter-scaled pattern. Young's modulus Y of 1.1 ± 0.2 kPa (soft) and 42.0 ± 1.1 kPa (stiff). (ii) "Double-rigidity" design, centimeter-scaled pattern. Y of 29.2 ± 1.1 kPa (soft) and 74.8 ± 2.8 kPa (stiff). (iii) "Stripes" design, micrometer-scaled pattern. Y (and stripe width) of 12 kPa (20 μm) (soft) and 40 kPa (5 μm) (stiff). Quantification of the substrate stiffness is presented as mean ± standard deviation (SD). (B) Pure glial or mixed neuronal−glial cell cultures are prepared from cortex or hippocampus dissociation from E18 mouse embryos. The cells are then cultured on fibronectin (FN) or poly-L-lysine/laminin (PLL+LN)-coated hydrogels with gradients of rigidity.

precisely, we analyzed the response of primary brain cells when cultured on multirigidity hydrogels with apposed areas characterized by two distinct values of compliance reminiscent of the variable compliance found in brain tissues,[31−33] in the presence of a stiffness-independent surface coating of either fibronectin or poly-L-lysine/laminine. The size of the stiffness patterns was tuned from the centimeter down to micrometer scale. In this way, we could compare cell responses to pairs of rigidity in identical culture conditions and shared soluble factors. Neuron and glial cell responses were systematically quantified as a function of the nature of the adhesive ligands immobilized on the surface of the hydrogel, of the composition of the culture medium, and of the cellular composition (pure glial cells versus standard dissociated brain tissue culture mixing neurons and glial cells). As main results, we first observed that, in accordance with previous studies,[11] the initial adhesion of neuronal cells is favored on soft compared to stiff substrates. We also observed that neurites' orientation on sharp stiffness gradients was similar to what was reported on smooth ones,[21] neurites orienting parallel to the gradient. Then, our main finding is that glial cells show a differential response to rigidity depending whether adhesive ligands are fibronectin or poly-L-lysine/laminin: adhesion and proliferation were enhanced on the stiff substrates when cultured on fibronectin, while soft substrates were preferred on poly-L-lysine/laminin coating. These observations, which were not dependent on mixed versus pure culture conditions, differ from previous reports.[11,26,30] This unique result was attributed to the improvement of the fabrication process of the culture support, which here allows for a coating of the adhesive ligands that is truly independent of the rigidity of the hydrogel. It then provides for the first time clues that some integrin subtypes may favor cell adhesion or proliferation on soft matrices.

2. MATERIALS AND METHODS

2.1. Substrate Fabrication and Characterization. Multirigidity polyacrylamide gels were fabricated using photopolymerization as described in reference 34. In brief, a photosensitive solution of polyacrylamide monomers was prepared using the UV-sensitive initiator bis(2,4,6-trimethylbenzoyl)-phenylphosphineoxide (Irgacure 819, Ciba). Irgacure 819 (2 mg) was dissolved in 10 μL of propylamine at 52 °C, just above the boiling point, for 10 min. Then, 490 μL of deionized water, 250 μL of a 40% solution of acrylamide, and 250 μL of a 2% solution of *N*,*N*-methylene-bis-acrylamide (Bio-Rad) were added, leading to a ratio of 10−0.5% of monomers. This photosensitive solution was exposed to 365 nm UV illumination through gray leveled masks engineered to spatially modulate the UV illumination and tune the rigidity profiles (Figure 1A). Several templates were chosen ("concentric" design, "double rigidity", and "stripes") that allowed exploring different ranges of stiffnesses and geometries.

Gray level masks were engineered using optical photolithography and etching on a microscope glass slide. The glass was first washed with a Piranha solution (H_2O_2:H_2SO_4) with a concentration ratio of 1:2 for 10 min. Then, 1 nm of titanium and the desired thickness of chromium were deposited onto the glass with a Plassys type electron gun. The thickness of the chromium layer determines the transmission coefficient of the gray level (Figure S1) and, consequently, the reticulation rate of the hydrogel.[35] An AZ1512HS resist (Clariant, Muttenz, Switzerland) was spun onto the metal deposit at 3000 rpm for 30 s to reach a 600 nm thickness. It was then illuminated through a black and white master lithographic mask that reproduces the patterns to be transferred in the hydrogel. The resist pattern was

https://doi.org/10.1021/acsabm.1c01295
ACS Appl. Bio Mater. XXXX, XXX, XXX−XXX

developed with a 1:1 AZ-developer:deionized water mixture for 1 min. Etching was performed in a DPS type etching reactor, using a chlorine:oxygen (2:1) plasma. The resist was removed by exposing it for 30 s to an oxygen plasma in the DPS reactor. The gray level mask was then rendered hydrophobic by grafting a fluorinated silane onto it. It was immersed into a 1‰ solution of Optool (DSX, Daikin, Pierre-Bénite, France) in perfluorohexane for 1 min and then allowed to react for 1 h in water vapor at 65 °C. It was then rinsed for 10 min in perfluorohexane. The gray level chromium mask was next fitted with 40 μm thick wedges on its edges.

Coverslips (30 mm diameter) were used as a support to the hydrogel. They were first cleaned in a 0.1 M NaOH solution for 10 min and then rinsed in deionized water followed by a bath in ethanol. The coverslips were then dried using dry air. A solution containing 484 μL of acetic acid and 56 μL of Bind-Silane (GE Healthcare, New York, USA) completed up to 15 mL with absolute ethanol was prepared. A 200 μL aliquot of this solution was pipetted to each coverslip and wiped off after a few tens of seconds with a dust-free wiper. This step was essential to allow stable, covalent bonding of the polyacrylamide hydrogels onto the glass coverslips.

A droplet of 30 μL of the photosensitive solution of polyacrylamide monomers was deposited onto an activated 30 mm coverslip and sandwiched with the gray level mask. UV illumination (Eleco UVP281, Gennevilliers, France, 2 W/cm^2) polymerized the polyacrylamide. The hydrogel was then gently detached from the gray level mask with tweezers after it was soaked into deionized water for 3 to 60 min, depending on the softness of the hydrogel. In this study, the exposure times and chrome thicknesses that we used to control the hydrogel rigidity were respectively 20 s and 29 nm for the millimeter-scaled rigidity pattern ("concentric" design, Figure 1A-i), 100 s and 39 nm for the centimeter-scaled rigidity pattern ("double rigidity" design, Figure 1A-ii), and 20 s and 14 nm for the micrometer-scaled rigidity patterns ("stripes" design, Figure 1A-iii). With this process, gels with thicknesses ranging between 25 and 30 μm were obtained.

Hydrogel stiffness was characterized by measuring the Young's modulus using atomic force microscopy in force mapping mode (NanoWizard II, JPK Instruments AG, Berlin, Germany). MLCT C tip cantilevers (Bruker, Santa Barbara, USA) with a nominal spring constant of 0.01 N m^{-1} have been employed for their ability to address Young moduli between 0.1 and 100 kPa (Figure 1A).

2.2. Polyacrylamide Coating and Characterization. Hydrogels were functionalized using Sulfo-LC-SDA photosensitive reagent (Sulfo-NHS-LC-Diazirine, Pierce Biotechnology, Waltham, USA). We employed fibronectin (FN, from human plasma, Roche Applied Science, Switzerland, ref 11080938001) or poly-L-lysine and laminin (PLL, P2636; LN, L2020, Sigma-Aldrich, St. Louis, USA). Hydrogels were first swollen overnight in deionized water. Covalent grafting of the FN was performed as follows: FN was first coupled to the heterobifunctional cross-linker sulfo-LC-SDA (Pierce, Waltham, USA) as described in reference 34. The hydrogel was then incubated with 300 μL of the solution of diazirine-coupled FN at a concentration of 80 μg/mL (FN coating) at room temperature. After 1 h, the solution was drawn off, and the hydrogel was immediately exposed to UV illumination (Eleco UVP281, 2 W/cm^2) for 5 min so that the diazirine function of the sulfo-LC-SDA binds to the surface of the polyacrylamide hydrogel. Covalent grafting of PLL and LN was performed in three steps. A 300 μL volume of a solution of sulfo-LC-SDA at concentration 0.44 mg/mL in water was deposited on the hydrogel for 2 h. The solution was then pipetted off, and the hydrogel was exposed to UV illumination for 5 min. A 300 μL aliquot of a solution of PLL at a concentration of 1 mg/mL was then incubated on the hydrogel for 1 h. After removal, 300 μL of a solution of LN at a concentration of 10 μg/mL was deposited on the hydrogel and left to react for 1 h. After these grafting steps, the hydrogels were rinsed three times in phosphate-buffered saline (PBS). This grafting protocol was shown to keep the rigidity of the hydrogel unchanged.[34]

The characterization of the surface coating was performed by immunostaining. The following antibodies and respective secondary antibodies were used in the indicated dilutions: polyclonal FN or LN antibodies (Sigma-Aldrich, St. Louis, USA, F3648 and L9393 at 1:400) and Alexa Fluor 488 conjugated donkey antirabbit (Thermo Fisher Scientific, Waltham, USA, 1:2000). Surface densities were quantified using confocal microscopy (Leica, Wetzlar, Germany, TCS SP2, objective 40× WI NA 0.6). Stacks of images were acquired in regions with different rigidities. In order to guarantee comparable acquisition conditions between stiff and soft areas, the intensity of the laser and the gain of the detector were maintained constant during all acquisitions. The stacks were prepared with identical numbers of images. The intensity signal was summed through every stack, and summed images were obtained. The summed images were then blurred with a disk of a 5 pixel radius to smooth the pixelated intensity signal. The mean intensity and the standard deviation were then calculated on the smoothed, summed images.

2.3. Primary Cell Culture. Cortical and hippocampal cells were obtained from embryos of 18 days of gestation of C57 BL/6J mice (Charles River, Wilmington, USA). The experiments in this study were approved by the local ethics committee. Dissociated brain tissue cultures were conducted as follows (Figure 1B): after dissection, cortices (including the hippocampus) were dissociated in DMEM medium supplemented with 10% fetal bovine serum (FBS, Thermo Fisher Scientific, Waltham, USA), 1% L-glutamine, 1% sodium pyruvate, and 0.05% peni-streptomycine (Thermo Fisher Scientific, Waltham, USA), a medium that we denote as DMEMs (supplemented DMEM). Cells were plated on the coated hydrogels at a 150 cells/mm^2 density. After 3 h, the culture medium was renewed, and cells were maintained either in neurobasal medium supplemented with 2% B27, 1% L-glutamine, and 0.05% penicillin−streptomycin (Thermo Fisher Scientific, Waltham, USA), referred to as NBs medium (supplemented NB) and known to optimize neuronal survival,[36] or in in DMEMs medium, which is the medium of reference for astrocyte cultures.[37] These cultures will be denoted as "mixed cultures" in this work, as they initially include neurons and, in a lesser proportion, glial cells. Pure glial cell cultures were conducted as follows (Figure 1B): after dissection and tissue dissociation, approximately 3 · 10^6 cells were plated per 100 mm Petri dish, previously functionalized with a poly-DL-ornithine coating (10 mL of a 1.5 μg/mL solution incubated overnight, P8638, Sigma-Aldrich, St. Louis, USA) and maintained in DMEMs. This medium improves glial cell proliferation whereas favoring neuronal death, thus leading to a pure glial cell population. DMEMs medium was renewed at 1 and 3 days in vitro (DIV). Cells usually reached confluence at 7 DIV. Cells were then gently detached after 0.05% trypsin−EDTA (Thermo Fisher Scientific, Waltham, USA) incubation at 37 °C, resuspended in DMEMs medium, and plated (30 cells/mm^2) on the coated hydrogel substrates. We observed that this density was low enough to limit physical contact in between astrocytes but high enough to ensure cell survival. Note that this density is much above the number of astrocytes plated in mixed cultures, as the proportion of astrocytes versus neurons for E18 mouse embryos is about 2−3%.[38] Consistently, we obtained a similar proportion of glial cells on FN or PLL/LN-coated hydrogels, where we quantified cell initial adhesion in serum-free NBs medium (Figure S2).

2.4. Immunofluorescent Stainings of Cells. Cells were fixed in 4% paraformaldehyde for 20 min and immunostained with the following antibodies and dilutions: actin was stained with phalloidin Alexa Fluor 594 (Thermo Fisher Scientific, Waltham, USA, 1:150) and DNA with Hoechst (Thermo Fisher Scientific, Waltham, USA, 1:1000).

2.5. Imaging and Image Analysis. Fluorescent images were aquired on an upright Olympus BX51 microscope at 10× magnification. Time-lapse acquisitions were performed at 10× magnifiation with a inverted microscope (Olympus, IX73) equipped with a heated workplate, a humidifier, a CO_2 delivery system, and a motorized stage to allow multiposition and multicondition acquisitions.

Cells were observed between 2 and 21 days in vitro (DIV) by maintaining the same samples in culture over the entire time span. Mean cell density values were calculated on a number of fields of view

https://doi.org/10.1021/acsabm.1c01295
ACS Appl. Bio Mater. XXXX, XXX, XXX−XXX

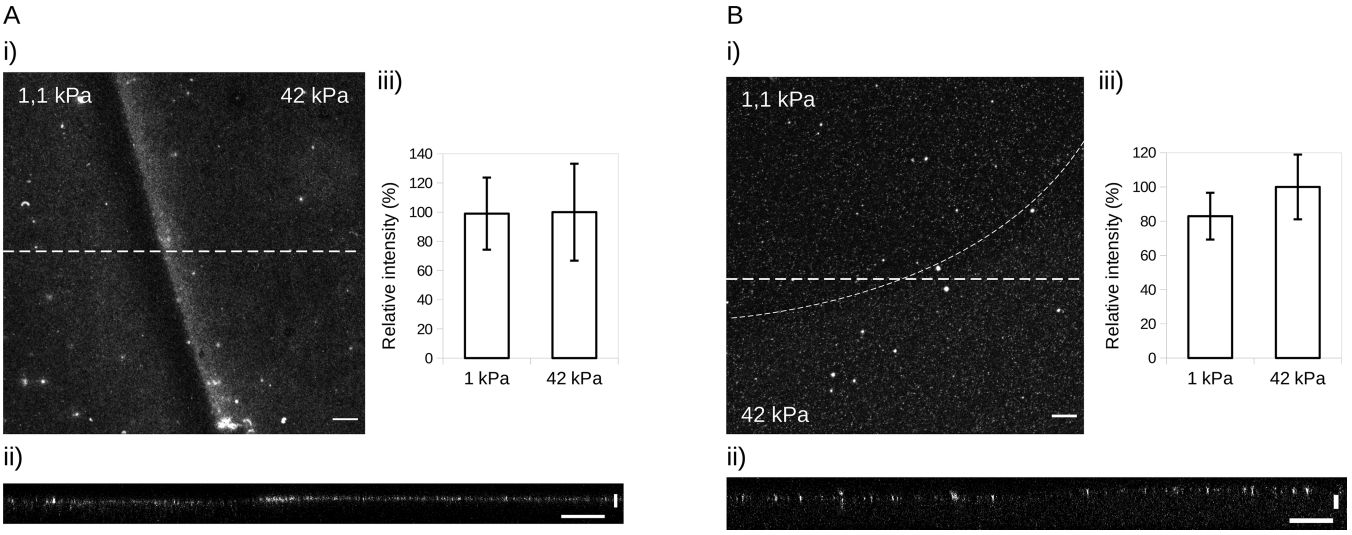

Figure 2. Surface density of the adhesive cues is independent of the rigidity. (A) Imaging of a stained "concentric" rigidity pattern with FN coating. (i) Sum of the confocal slices of the stack. (ii) In-depth projection of the surface density along the dashed line in (i) shows identical intensity on the left (soft) and the right (stiff) sides of the frontier. (iii) Quantification of the intensity of the staining in the soft and the stiff regions. (B) Same as (A) for PLL/LN coating. Horizontal bars: 30 μm. Vertical bars: 10 μm.

(surface of around 0.5 mm^2) varying from 4 to 12 and depending on the localization of the area of interest in the sample. Identification of the region (stiff vs soft) was made possible, as the border between them was either brighter or darker than the surroundings in phase contrast microscopy. Cell counting was performed by identifying cell nuclei on the phase contrast images (Figure S3). This method was preferred to the live imaging of an internalized fluorescent dye, as the focus was on measuring the proliferative capacity of the cells. Since live imaging of fluorescent dyes are more and more disputed because of their phototoxicity and side effects on cell cycle,[39] unavoidable uncertainties in cell counting due to the difficulties to identify individual cells were preferred to uncontrolled biases induced by internal fluorescent dye. Cell counting was performed three times on every image at distant times to limit systematic biases in cell counting. Repeatability in cell counting was better than 97%. As shown in Figure S3, the identification of individual cells at low cell density was fairly straightforward, as the nuclei were easily identifiable. Nuclei in high density cell layers were identified by their gray level footprints. Differences of contrast along the cell contours were also used to identify individual cells. In case of a doubt, the counter was not incremented; thus, we anticipate that our counting may underevaluate the true number of cells in the dense monolayers. Fields of view were always chosen in diametrically opposed positions on the circular shape of the gel, in order to get representative descriptions of cell distribution. This corresponds to an amount of counted cells from a few tens to more than 2000 (in cases of high proliferation). This method was validated on a fixed sample where the number of cells identified on phase contrast images was compared to the Hoechst staining. This allowed to estimate the mean error of 3% (Figure S3).

Neurons and glial cells were quantified after a medium change and, thus, after dead cell removal. Both cell types were identified by their morphology from phase contrast images. Other cell types, for instance microglia, were distinguished, and therefore discarded, by their shape and fast dynamics (Figure S4).

Gels with identical stiffness characteristics and uniform coatings were used to compare the effects of coating and culture conditions. The processing of the "concentric" design, with a large area with a Young's modulus of 1 kPa, was difficult to obtain as cracks easily formed. Stiffness reproducibility was also difficult to achieve in this range of values. To limit bias, quantitative analysis was only performed on gels without fractures, as the latter indeed locally change the mechanical properties of the gel (making it harder) and the coating density (making it more concentrated). Eight intact gels with identical mechanical feature were obtained, allowing to reliably compare all the conditions. Other gels showing local defaults or larger stiffnesses were used as qualitative controls (n = 1 to 9 depending on the conditions).

2.6. Data Analysis and Statistical Analysis. The initial cell adhesion is calculated as the cell density at the first day of observation (2 DIV for pure cultures) normalized by the seeding cell density. The proliferation rate is calculated within a temporal range $\Delta t = t_i - t_0$. The number of cell divisions n is obtained by the following equation: $N(t_i)/N(t_0) = 2^n$, where N is the average cell density. The mean cell surface is calculated by dividing the total area of confluent cells (i.e., computed from fields of view with no cell-free surfaces) by the number of adherent cells. Statistical analyses and linear regression were carried out with GraphPad Prism software. A Mann−Whitney test (two-tailed, unpaired, with a significance level of 0.05) was performed between two groups of non-normal data.

3. RESULTS

3.1. Generation of Multirigidity Substrates. In order to address the sensitivity of primary brain cells to rigidity and gradients of rigidity, we used a gray leveled lithography technique based on an optimized photochemistry dedicated to the design of polyacrylamide hydrogels.[34] This enhanced photochemistry is carried out by activating the very efficient photoinitiator bis(2,4,6-trimethylbenzoyl)-phenylphosphineoxide (Irgacure 819, Ciba) dispersed in water by the use of propylamine in the vapor phase (see Materials and Methods). Compared to the 2-hydroxy-4′-(2-hydroxyethoxy)-2-methylpropiophenone (Irgacure 2959, Ciba) more often utilized for the polymerization of water-soluble polymeric materials,[40] this allows sharp gradients of rigidity to be printed in polyacrylamide hydrogels. Centimeter-, millimeter-, and micrometer-scaled regions can then be apposed with sharp transitions of several kPa/μm (Figures 1A and S5). For our purpose, millimeter- and micrometer-sized patterns were designed to analyze the initial adhesion of primary neurons and glial cells, neuronal growth, and glial cell proliferation with different pairs of rigidity conditions, e.g., 1 and 42 kPa; 29 and 75 kPa; and 12 and 40 kPa. These values were chosen relative to the wide distributions of stiffness values found in brain tissues:[31−33] while mean values stand between 0.5 and 3 kPa,[41,42] individual cells may face much stiffer environments

https://doi.org/10.1021/acsabm.1c01295
ACS Appl. Bio Mater. XXXX, XXX, XXX−XXX

for instance in the presence of a dense network of extracellular matrix,[43] along vessel walls or myelinated fibers.[44−46] Combined effects of the surface coating (FN versus PLL/LN), culture conditions (pure glials versus mixed neuronal−glial cell cultures), and culture media (DMEMs or NBs) were analyzed on these multirigidity substrates (Figure 1B).

3.2. Density of the Surface Coating on the Hydrogel Is Independent of Rigidity Gradients. Proteins from the ECM were coated at the surface of the polyacrylamide hydrogels to ensure cell adhesion, as bare polyacrylamide hydrogels are not permissive substrates. Fibronectin and laminin were chosen, as these are the most widely used proteins for in vitro testing. These proteins are found in the brain extracellular matrix, mainly in the neural interstitial matrix and in the basement membranes along blood vessels.[47] Poly-L-lysine was also used in combination with laminin, as it is often employed in an in vitro neuronal culture, either alone or in combination with laminin, to enhance the adsorption of the proteins from the culture medium.[30,48,49] We could check that the surface density of the adhesion proteins did not show any significant variations with the rigidity even in the regions where the gradient of rigidity is of the order of a few kPa/μm (Figures 2 and S6). Topography was observed on centimeter- and millimeter-scaled rigidity patterns in the place of the gradient of rigidity (Figure 2). The transition zone between soft and stiff large areas (millimeter- to centimeter-scaled) displayed a smooth topography consisting in a step of at most 5 μm over a length of 8 μm, associated with an enhanced functionalization (Figure 2A). Both effects could influence cell positioning, and for this reason, the frontiers were not considered in cell counting. Finally, no topography nor enhanced coating density were observed on micron-scaled patterns of rigidity (Figure S6).

3.3. Neuron Initial Adhesion Depends on the Rigidity whereas Survival Does Not. We then investigated brain cell adhesion and proliferation on the millimeter-scaled patterns. Neuron sensitivity to rigidity was probed on the "concentric" patterns with Young's moduli of 1.1 ± 0.2 kPa (soft) and 42.0 ± 1.1 kPa (stiff) (Figure 3A−D). Neuron initial adhesion and survival until 17 days in vitro (DIV) were analyzed from cells grown in mixed cortical culture in NBs in the absence of serum as described in the Materials and Methods. Poly-L-lysine/laminin (PLL/LN) coating was employed to ensure neuron adhesion, as fibronectin (FN) did not allow proper neuronal adhesion and growth (Figure S7). For instance, Figure S7 reports an example of aggregates of neurons produced on the FN coating, where cell counting was thus not possible. On the PLL/LN-coated gels, it was observed that although the amount of adherent neurons was slightly but significantly larger on the soft substrates than on the stiff ones (Figure 3C), neuron density on both rigidities appeared statistically constant over the entire time span. This shows that neuron survival is independent of the rigidity of the substrate. The slight variations in the number of neurons over time were attributed to the difficulty to count them in phase contrast images, especially after 2 weeks of culture when neurons are organized in mature networks and where individual somas can be difficult to identify (Figure S3).

3.4. Neurites Grow Preferentially Parallel to kPa/μm Gradients of Rigidity. The orientation of the neurites at the border between the stiff and the soft regions was quantified by analyzing the phase contrast images of mixed cortical cultures grown on a "double rigidity" pattern, with Young's moduli of

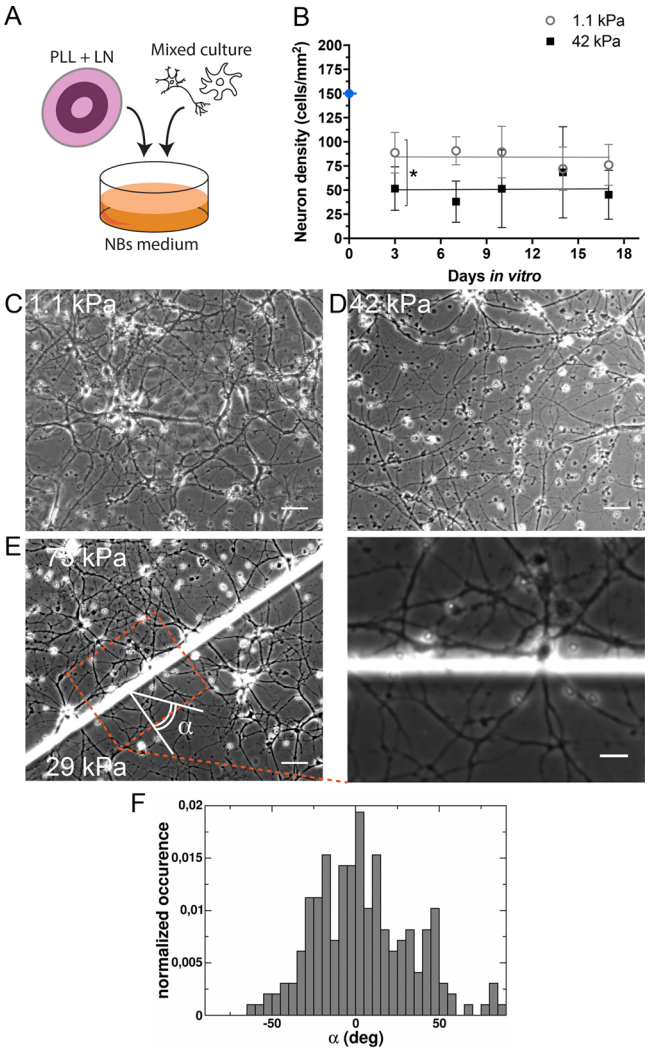

Figure 3. Neuronal cell growth in mixed cultures on laminin/poly-L-lysine-coated substrates in NBs culture medium. (A) Schematics of the cell culture conditions for (B−D). (B) Neuron density and its evolution over time (DIV) on stiff (black squares) and soft (white circles) regions. The blue dot indicates the initial cell concentration seeded on the substrate (including both glial and neuronal cells). Quantification of the cell density is presented as mean ± standard deviation (SD). *, p (stiff vs soft) = 0.0380 (3 DIV). Slopes not statistically different from zero: p (soft) = 0.1502; p (stiff) = 0.6781. The gray and black lines in the graphs show the linear fit between 6 and 17 DIV. (C,D) Phase contrast imaging of neuronal cells on soft (C, 1.1 kPa) and high stiffness (D, 42 kPa) on a "concentric" pattern of rigidity at 14 DIV. Scale bars: 50 μm. (E) Phase contrast imaging of neurons at the frontier between the low and the high stiffness regions on the "double rigidity" design. Right: zoom of the region in the red dashed square on the left. Scale bars: 50 μm and 20 μm (zoom). (F) Neurite orientation at the frontier between the soft and the stiff regions, characterized by the angle α perpendicular to the frontier as shown in E. The histogram for α is centered at 0°.

29.2 ± 1.1 and 74.8 ± 2.8 kPa (Figure 3E,F). We observed that the neurites predominantly cross the rigidity border perpendicular to it, thus aligning with the gradient of rigidity (Figure 3E,F). However, the direction of the growth of the neurites (i.e., from soft to stiff, or the opposite) could not be deduced from the images, due the large surface density of the cells.

https://doi.org/10.1021/acsabm.1c01295
ACS Appl. Bio Mater. XXXX, XXX, XXX−XXX

3.5. Glial Cell Initial Adhesion and Proliferation in Pure Cultures Are Favored on High Rigidity in the Presence of Fibronectin Coating. As glial cells do not adhere nor proliferate properly in culture conditions that are favorable to neurons (PLL/LN coating and NBs culture medium, Figure S2B), glial cells' sensitivity to rigidity was first evaluated in pure culture conditions. Glial cells were seeded on fibronectin (FN)-coated "concentric" rigidity patterns characterized by Young's moduli of 1.1 ± 0.2 kPa (soft) and 42.0 ± 1.1 kPa (stiff) and cultured in DMEMs, the referenced medium for this culture[37] (Figure 4A). The cell density was measured from 2 to 17 DIV. We observed an almost absence of cells on the soft region during the entire time span (Figure 4B). Residual cells mostly remained round and did not spread. Conversely, on the stiff regions, the initial cell density of seeding (around 30 cells/mm^2) was conserved after plating, as observed at 2 DIV, showing that the combination of a 42 kPa stiff substrate and FN coating supports the initial adhesion and growth of glial cells. The proliferation rate was close to constant between 2 and 8 DIV, with an averaged value of 0.27 (Figure 4B). Furthermore, the glial cells were widely spread on the stiff regions (mean cell surface: 14.5 ± 3.4 · 10^3 μm^2, Figure 4C). Confluence was reached between 8 and 17 DIV, at a plateau of cell density of 60 ± 22 cells/mm^2 on average.

3.6. Glial Cell Rate of Proliferation Is Dependent on the Culture Medium and of the Presence of Serum. In order to study the impact of the culture medium and of the serum, glial cells from pure culture conditions were grown as above on "concentric" 1.1−42 kPa rigidity patterns coated with FN coating but using NBs as the culture medium instead of DMEMs (Figure 4D). In order to adhere, the cells were first grown for 24 h in DMEMs medium. DMEMs was then replaced by NBs for the following days. As above, a weak adhesion and a poor survival were observed on the soft region. Contrarily to Figure 4C, Figure 4E shows that the proliferation rate on the stiff region is almost null, the slope of the cell density over the time between 2 and 17 DIV being insignificantly different from 0 (p = 0.5366). Thus, the culture medium, including the presence of serum, is critical to obtain a significant rate of proliferation on the stiff substrate.

3.7. Changing Fibronectin Coating to Laminin/Poly-L-lysine Reverses Glial Cell Response to Rigidity. The surface coating was changed to PLL/LN, a surface coating that is less favorable to glial growth.[37] Glial cells were grown on an identical pattern of rigidity as above using pure culture conditions in DMEMs (Figure 5A). Strikingly, the dependence on the rigidity of the glial cell initial adhesion and proliferation was reversed using PLL/LN instead of FN (Figures 5C and 7A,B). Indeed, only rare cell adhesion and almost no proliferation were observed on the stiff regions (Figure 5B,C). Conversely, cells adhered on the soft regions, and a weak but significant cell proliferation was measured, associated with widely spread morphologies similar to those observed on FN coating on stiff regions (mean cell surface: 14.3 ± 4.3 · 10^3 μm^2). The cell proliferation rate on the soft regions displayed a value of 0.4 between 2 and 6 DIV. After 6 DIV, cell density reached a plateau associated with a cell confluence of approximately 60% (Figure 5C). We investigated whether this observation was conserved in a different culture condition. Mixed cortical cultures were thus grown on identical culture supports as above in DMEMs (Figure 5D). In this condition, characterized by a very small initial proportion of glial cells compared to neurons (about 2−3%[38]), we also observed that

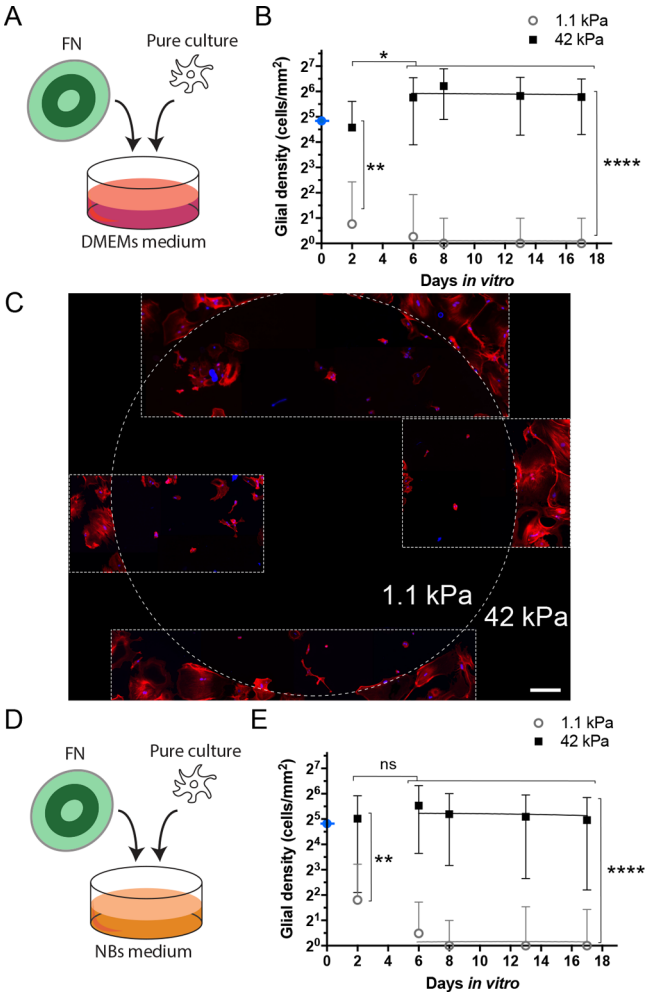

Figure 4. Glial cell initial adhesion and proliferation in pure cultures on fibronectin-coated substrates. (A) Schematics of the cell culture conditions for (B,C). (B) Evolution of the cell density in DMEMs medium over time (days in vitro, DIV) on stiff (black squares) and soft (white circles) regions. **, p (stiff vs soft) = 0.0050 (2 DIV); ****, p (stiff vs soft) < 0.0001 (6 to 17 DIV); the cell number remains stationary between 6 and 17 DIV (p = 0.6463), and * denotes that it is significantly increased between 2 DIV and 6 to 17 DIV on stiff (p = 0.0187). (C) Immunofluorescence images of a glial cell culture in DMEMs medium: the frontier (white dashed line) delineates the soft, inner region and the stiff, outside area. The delineated white rectangles mark out the immunofluorescence images in the rigidity pattern. Red: phalloidin, actin. Blue: Hoechst, nuclei. Cells are fixed at 12 DIV. Scale bar: 300 μm. (D) Schematics of the cell culture conditions for (E). (E) Evolution of the cell density in NBs medium over time, with identical conventions as in B. **, p (stiff vs soft) = 0.0094 (2 DIV); ****, p < 0.001 (6 to 17 DIV). Here, the cell density is not significantly increasing in the stiff region (ns, p = 0.6207 between 2 and 6 DIV). The gray and black lines show the linear fit between 6 and 17 DIV. The blue dots indicate the initial cell concentration seeded on the substrate. Quantification of the cell density is presented as mean ± standard deviation (SD).

the PLL/LN adhesive coating promotes a larger proliferation rate of glial cells on soft substrates than on stiff ones (Figures 5F and 7B). However, contrarily to the case of pure culture, a nonzero proliferation rate was observed on stiff regions.

3.8. Glial Cell Initial Adhesion and Proliferation in Mixed Cultures Show an Enhanced Response to Rigidity Compared to Pure Culture, Associated with

https://doi.org/10.1021/acsabm.1c01295
ACS Appl. Bio Mater. XXXX, XXX, XXX−XXX

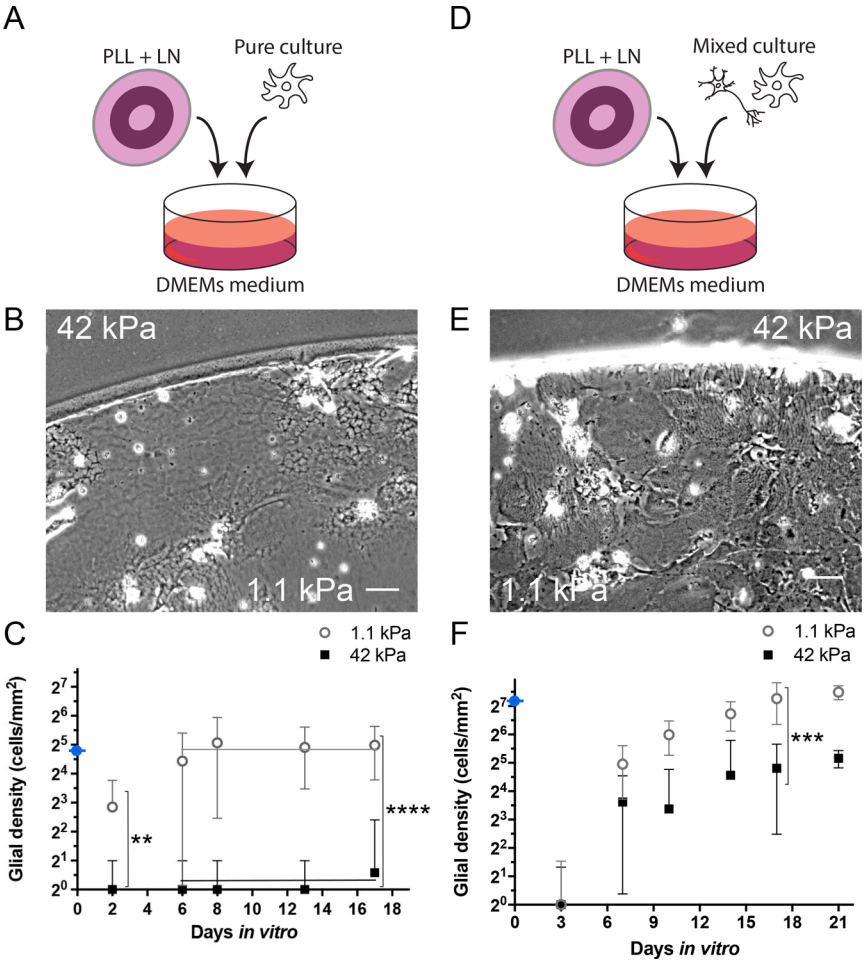

Figure 5. Glial cell initial adhesion and proliferation on poly-L-lysine/laminin-coated substrates in DMEMs culture medium. (A) Schematics of the cell culture conditions for (B,C). (B) Glial cells from pure culture at the stiff (42 kPa)−soft (1.1 kPa) frontier on a "concentric" pattern of rigidity at 17 DIV. (C) Evolution of the cell density over time on stiff (black squares) and soft (white circles) regions. **, p (stiff vs soft) = 0.0016 (2 DIV); ****, p (stiff vs soft) < 0.0001 (between 6 and 17 DIV). Cell density does not vary significantly between 6 and 17 DIV. The gray and black lines show the linear fit between 6 and 17 DIV (slope not significantly different from zero, p = 0.1946 (stiff) and 0.4699 (soft)). (D−F) Idem for glial cells from mixed culture (phase contrast image at 17 DIV). ***, p (stiff vs soft) = 0.003. The blue dots indicate the initial cell concentration seeded on the substrate (including both glial and neuronal cells for the mixed culture). Quantification of the cell density is presented as mean ± standard deviation (SD). Scale bars: 50 μm.

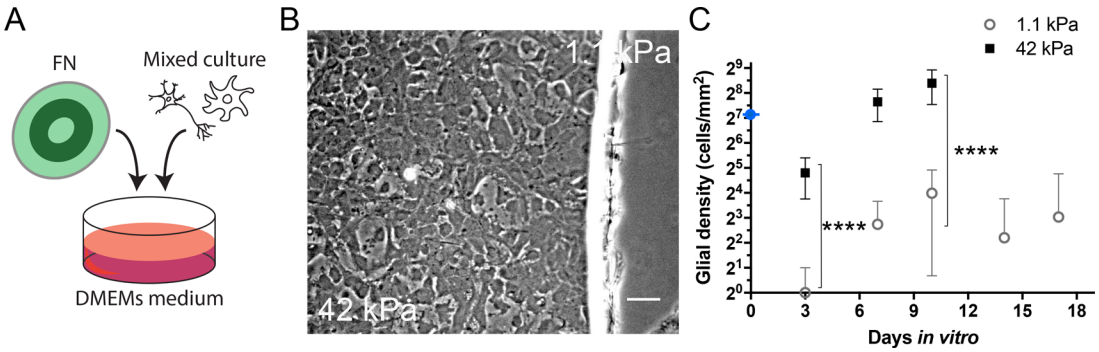

Figure 6. Glial cell initial adhesion and proliferation in mixed cultures in DMEMs medium on fibronectin coating. (A) Schematics of the cell culture conditions for (B,C). (B) Phase contrast imaging of glial cells at the border of stiff (42 kPa) and soft regions (1.1 kPa) at 21 DIV of a "concentric" pattern of rigidity. Scale bar: 50 μm. (C) Evolution of the cell density over time (DIV) on stiff (black squares) and soft (white circles) regions. ****, p (stiff vs soft at 3 and at 10 DIV) < 0.0001. The blue dot indicates the initial cell concentration seeded on the substrate (including both glial and neuronal cells). Quantification of the cell density is presented as mean ± standard deviation (SD).

Limited Spreading. The proliferation rates of glial cells from pure and mixed culture conditions were both enhanced on the soft region on PLL/LN coating (Figure 5). However, quantitative differences in the initial cell adhesion or cell proliferation rates were observed (Figure 7). We therefore investigated whether glial cell initial adhesion and proliferation

https://doi.org/10.1021/acsabm.1c01295
ACS Appl. Bio Mater. XXXX, XXX, XXX−XXX

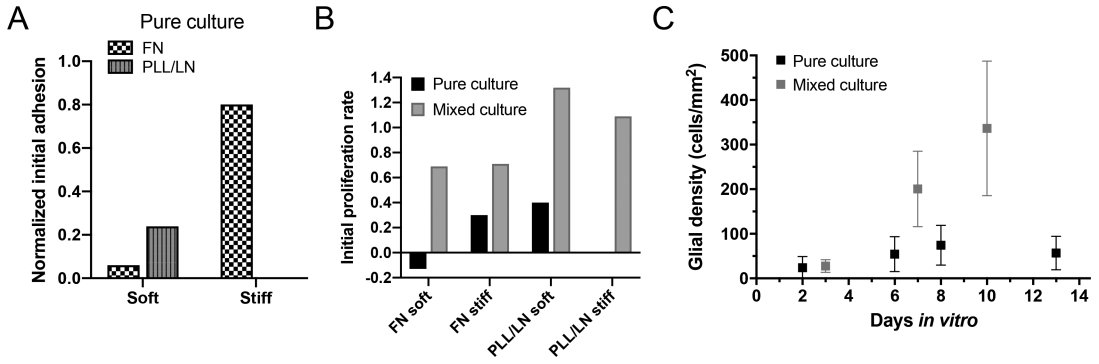

Figure 7. Rigidity sensitivity of glial cells from mixed cultures in DMEMs is enhanced compared to pure cultures. (A) Comparison of the normalized initial adhesion of glial cells from pure cultures on the different coatings ("FN": fibronectin, "PLL/LN": poly-L-lysine/laminin) and rigidities ("Soft": 1.1 kPa, "Stiff": 42 kPa). (B) Normalized initial proliferation rates show that glial cells proliferate faster in mixed culture conditions. (C) Comparison of the evolution of the cell density in pure and mixed cultures on the stiff regions coated with FN.

would be enhanced by the presence of neuronal cells also on FN coating, even if neurons do not survive for long in these medium and coating conditions. Cells were grown on the "concentric" pattern with FN coating and DMEMs culture medium (Figure 6A). This resulted in glial cell proliferation and progressive neuronal death. As in pure glial cultures, glial cells in mixed cultures adhered preferentially on stiff regions (Figure 6B), with the initial cell density at 3 DIV being larger by a factor of more than 20 on the stiff than on the soft regions (Figure 6C). We compared the rates of glial cell proliferation depending on the culture conditions (Figure 7B). We first observed that mixed culture conditions are more favorable to glial cell initial adhesion: while almost no cells from pure culture conditions adhere in the presence of an unfavorable rigidity (soft on FN, stiff on PLL/LN), a small number of adherent glial cells from mixed culture conditions is sufficient to reach a significant proliferation rate in all conditions (Figure 7B). Indeed, the proliferation was enhanced for all coatings and rigidities in mixed culture conditions compared to pure cultures (Figure 7B,C). This led to very dense layers of cells on the stiff regions coated with FN, with their mean surface going down to $3.3 \pm 1.8 \cdot 10^3$ μm^2, more than 4-fold smaller than in pure culture conditions. However, this large rate of proliferation and cellular compaction led to the detachment of entire portions of the cell monolayer, causing the impossibility to count cells later than 10 DIV (Figure 7C). We conclude that the initial presence of neurons therefore enables enhanced initial cell adhesion in all conditions and favors cell proliferation. This observation could however not be extended for cells cultured in NBs. As in a pure glial culture, the use of NBs instead of DMEMs did not allow to maintain a detectable proliferation of glial cells, independent of the stiffness and the nature of the adhesive coating (Figure S2).

3.9. Glial Cells Adapt Their Shape to Subcellular Rigidity Gradients but Do Not Get Confined. Unlike the macroscopic rigidity patterns, micrometer-scaled patterns of rigidity do not show topography nor variations of the coating density in the regions with large gradients of rigidity. We thus wondered how these cellular- or subcellular-scaled patterns of rigidity would impact cell adhesion and shape and whether the cells could get confined by the gradients of rigidity as other cells do (see Figure S8). For this purpose, glial cells from pure culture conditions were grown on a parallel array with alternated soft and stiff areas at a scale similar to the cellular sizes (Figure 1A-iii). More precisely, stiff stripes of width between 5 and 75 μm were alternating with soft stripes with widths in between 20 and 50 μm. A uniform FN coating and DMEMs medium were used for this study, to optimize the initial cell adhesion and to culture cells in proliferating conditions. We observed that single glial cells got deformed by the rigidity patterns (Figure 8, pattern of 5 (stiff)−20 (soft) μm stripes). They preferentially extended lamellipodia on the stiff stripes. But we did not observe cell confinement on the patterns as for other cell types (Figure S8), even when enlarging the distance between the stiff stripes (Figure S9).

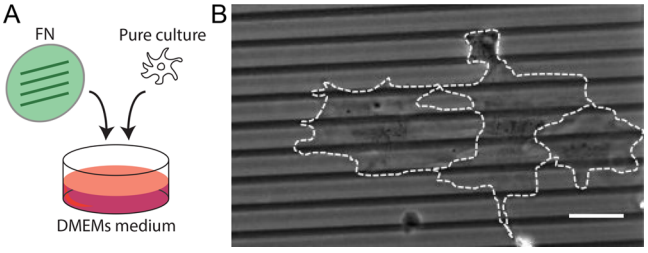

Figure 8. Glial cells are deformed by subcellular rigidity patterns. (A) Schematics of the cell culture conditions. (B) Representative image showing glial cells on the stiffness microgratings. Stiff stripes of 5 μm, 40 kPa, appear darker and alternate with soft stripes of 20 μm, 12 kPa, 2 DIV. White dashed lines delineate cell contours. Scale bar: 50 μm. Other designs of the rigidity pattern can be found on Figure S9.

4. DISCUSSION

Using functionalized multirigidity polyacrylamide hydrogels, we have investigated the combined response of primary brain cells to the stiffness and chemical coating of their extracellular matrix. This technique has proved to be a unique tool to probe cellular responses to a panel of rigidities under identical culture conditions in terms of culture medium, adhesive molecules, and soluble cues secreted by the cells. Two types of culture media have been tested, one more favorable for glial cells (serum-rich DMEMs), the second one designed for hippocampal neuron survival (NBs, serum-free medium). Two coatings have been tested, based on two important components of the ECM in the brain: fibronectin (FN) and laminin (LN, associated with poly-L-lysine, PLL).[47] In this study, two types of initial cell preparations have also been investigated, purified glial cell suspension or dissociated

https://doi.org/10.1021/acsabm.1c01295
ACS Appl. Bio Mater. XXXX, XXX, XXX−XXX

cortical tissue, to test the influence of neurons on glial cells' mechanosensitivity.

First, we confirmed that embryonic neurons in mixed cultures adhere better on softer supports[11] (Figure 3). We then observed that their survival is not sensitive to the stiffness of the matrix (Figure 3B). This observation differs from reference 11, where neurons on the stiff polyacrylamide hydrogel (27 kPa) were mostly observed over glial cells and not directly on the stiff hydrogel itself. Here, glial cells sparsely survived either on the soft or the stiff regions in these culture conditions (NBs medium, absence of serum, PLL/LN coating) (Figure S2B), while neuron density remained significant on both regions (Figure 3). Differences of more than an order of magnitude of the surface density of the coating may be at the origin of this distinct behavior; the viability of neurons being dependent on laminin density.[50] Nevertheless, consistent with references 11 and 20, we qualitatively observed a slightly lower density of neurites on the stiff than on the soft regions (Figure 3C,D). Analysis of the orientation of neurite growth relative to the orientation of the rigidity gradient showed that neurites align perpendicular to the border between the stiff and the soft regions and thus parallel to the gradient of rigidity (Figure 3E,F). Previous studies had already reported on neurites' sensitivity to rigidity. References 17, 21, 51, and 52 reported that neurite length depends on the rigidity of the extracellular matrix and that the length is further modulated by the coating.[17] In addition, neurites were reported to grow from stiff to soft,[21,52,53] parallel to the gradient of rigidity.[52,53] Different from references 17 and 21, we could however not confirm that neurite growth is identical on FN and PLL/LN as neurons cultured on FN coating grew on top of glial cells and arranged as 3D aggregates (Figure S7).

Concerning glial cells, we first observed that glial cell initial adhesion and proliferation on FN is favored on the stiff regions as already reported on other surface coatings[11,26,30,54] (Figures 4 and 6). However, unexpectedly, PLL/LN coating led to larger initial adhesion and proliferation rates on soft regions compared to the stiff ones (Figures 5). The difference in cell numbers between the soft and rigid regions was very large, with a 30-fold increase in cell density on the soft part of the substrate compared to the rigid part. Such a large difference could not be attributed to errors in cell counting. This observation was shown to be independent of the cell preparation, glial cells being either purified from neurons before seeding or seeded as cortical, mixed cultures (Figure 7, $n = 2$ for each cell preparation). The combination of PLL and LN had never been tested before. And this surprising organization of the glial cells was observed on multirigidity substrates, meaning that soluble cues could be shared between the stiff and soft conditions (Figure 2). It differs from other studies conducted on substrates with uniform stiffness, coated either with LN alone,[11] poly-D-lysine (PDL),[26,30] or PLL.[54] Several factors could explain this difference. First, coating protocols often result in an involuntary correlation of the surface density of the adhesive ligands and the stiffness of the hydrogel, softer hydrogels having a lower surface density of ligands than stiffer ones.[34] This experimental pitfall is reported in reference 30 and was assumed to only result in a delay in glial cell initial adhesion and proliferation.[30] This assumption is questionable, as cell adhesion and proliferation were shown to depend on the surface density of the coating for other cell types.[55] Here, much attention was paid to achieving a uniform surface coating (Figure 2), which appeared to be very sensitive to the hydration of the surface of the hydrogel. Indeed, the protocols we use here or that were used in the aforementioned studies consist in the covalent binding of the adhesive ligands to the surface of the hydrogel through the grafting of a UV-activated cross-linker (sulfo-SANPAH or sulfo-LC-SDA).[56] Only the cross-linkers that are in the close vicinity of the surface of the hydrogel may bind to the hydrogel after UV exposure, as the free radicals are very unstable and recombine with water. After incubation, the solution of cross-linkers is drawn off the hydrogel before UV exposure. The wet film at the surface of the hydrogel dehydrates in air, which concentrates the cross-linkers to its surface. But the rate of dehydration is sensitive to the porosity (and therefore the stiffness) of the hydrogel,[57] which may result in a stiffness-dependent concentration of cross-linkers at the surface of the hydrogel. Here, we took care of exposing the hydrogel to UV immediately after the withdrawal of the cross-linker solution, within a delay of few seconds. This limited dehydration resulted in a coating that was fairly independent of the local stiffness (Figure 2), while too long of a delay before UV exposure always led to nonuniform surface coating, the stiffer regions bearing a larger surface density of adhesive ligands (Figure S10). In this latter condition, cells are expected to poorly adhere to the soft regions, and the effect we report cannot be observed.

Another reason why this effect has not been seen may come from the chemical nature of the coating, of PLL/LN. References 26, 30, and 54 used PDL or PLL alone as a coating of the soft matrix. These are known to facilitate cell initial adhesion by the unspecific, electrostatic attraction of the cells.[30] But they also additionally induce a dominant secretion of FN by the cells, compared to LN,[58] thus leading to conditions that resemble the FN coating. In contrast, in our study, PLL is saturated with LN. Therefore, initial adhesion is conditioned by this coating. The adhered cells may then still secrete FN; nevertheless, the interaction of rat embryonic cells with the substrate, in terms of morphology or migration, was shown to differ noticeably from the one observed on a FN coating.[59] These results are in line with our observation that the presence of LN makes profound changes in cell/matrix mechanical interaction.

Another reason for obtaining reversed stiffness sensing with glial cells may arise from the fact that our experiments are conducted on a multirigidities substrate. Soluble factors that the cells secrete on every stiffness are shared to all the cells. The role of soluble factors can be seen when comparing pure and mixed culture conditions. Glial cell proliferation is enhanced by the presence of the neurons, even in conditions that are not prone to neuron survival (Figure 7). This behavior may be induced by factors secreted by neurons, which have been shown to enhance cortical gliogenesis in early stages.[60] Another hypothesis is that their progressive death in DMEMs medium may act as a trigger of glial cell proliferation, as suggested by reference 61.

Finally, we observed that stiffness micrograting did not allow the glial cell bodies to be confined (Figures 8 and S9), contrary to other cell types (Figure S8). This unusual cell behavior was obtained on FN coating and DMEMs medium, which are culture conditions favorable to cell adhesion and growth. This qualitative observation further illustrates that glial cells have a very specific response to stiffness. Studying their proliferation on substrates with uneven stiffness at the subcellular scale could then provide more insights into how

https://doi.org/10.1021/acsabm.1c01295
ACS Appl. Bio Mater. XXXX, XXX, XXX−XXX

glial cells balance the differential proliferation rate we report between soft and stiff conditions for larger-scale heterogeneities in stiffness.

In line with our observation of reversed cell sensitivity to the rigidity of the matrix on the PLL/LN coating, a recent work reports on the enhancement of astrocyte activation in a soft environment,[62] different from previous studies that reported on increasing activation with the stiffness of the extracellular matrix.[26,54] This difference was attributed to the nature of the chemical coating, collagen 1. On collagen 1, glial cells also adopted a round morphology on the stiff substrate and an elongated shape with well-formed actin fibers on the soft substrate, similar to our study. Glial cell activation could be recovered on the stiff substrate with lowering the cytoskeletal tension by the use of blebbistatin.

Cell proliferation, on which we focus here, is also regulated by the cytoskeletal tensions and involves the buildup of cellular tractions forces on the substrate.[63] But LN and FN coatings do not involve the same integrins, which results in different capabilities of raising traction forces. For instance, $\alpha_6\beta_1$ integrins, which are involved in cell adhesion on LN,[64] were shown to build up traction forces of smaller amplitude than $\alpha_5\beta_1$ integrin, which interacts with FN.[65] Focal adhesions and stress fibers were also shown to be significantly reduced on LN compared to FN.[66] Moreover, LN was shown to involve a different signaling pathway than FN for the mechanosensitivity of neurons.[14] The existence of an optimal stiffness for cell proliferation was evidenced in several cell lines,[55] as well as the existence of an optimal coating density.[67] This optimum was interpreted as resulting from the balance between the kinetics of reinforcement of the adhesive machinery of the cell that makes the link with the substrate (the clutches) and the kinetics of the increase of the strain in the clutches because of the activity of the myosin motors.[18,68] In the motor-clutch model, a decreased collective resistance of the clutches, due to a limited number of clutches, a slower kinetics of the binding of the clutches, or a lower individual resistance to strain shifts the optimal stiffness for traction forces to a lower value.[68] Then, the mechanically less robust adhesion that takes place on LN coating could be at the origin of a softer optimal stiffness for glial cell proliferation compared to FN.

Based on recent works in mesenchymal stem cells that evidenced that distinct proteins of the extracellular matrix differently modulate the translocation of the YAP/TAZ transcriptional factor from the cytoplasm to the nucleus and that cell response on LN is specific compared to FN, collagen I, or collagen IV,[69] it would be of interest to address the YAP/TAZ translocation in primary glial cells on LN coating compared to FN. YAP/TAZ translocation is intimately related to cell response to stiffness[70] and could provide mechanistic information on this unexpected enhanced proliferation on PLL/LN-coated substrates with 1 kPa.

5. CONCLUSION

In conclusion, by using a recent technique of hydrogel photopolymerization that allows stiffness texturing to be achieved with sharp gradients, of a few kPa/μm, and to independently guarantee a uniform coating of adhesive ligands, we observed for the first time that glial cell initial adhesion and proliferation respond in a coating-dependent manner to the local stiffness of the matrix. Cell culture on fibronectin coating was shown to favor cell initial adhesion and proliferation on the stiffer regions of the matrix, of the order of 40 kPa, while the combination of poly-L-lysine and laminin would favor cell initial adhesion and proliferation on the softer parts of the substrate, of the order of 1 kPa. This reversed sensitivity to stiffness induced by the chemical nature of the coating was interpreted as the result of a difference in the contractility capabilities of the glial cells in dependence on the coating, which results in a shift in the optimal stiffness for cell proliferation.

■ ASSOCIATED CONTENT

Supporting Information

The Supporting Information is available free of charge at https://pubs.acs.org/doi/10.1021/acsabm.1c01295.

Figures S1−S10: Light transmission through chromium layers; Initial adhesion and proliferation of glial cells from mixed culture conditions in NBs culture medium for different surface coatings; Identification of cell nuclei on phase contrast images; Microglial cells on hydrogels; Comparison of the efficiency of Irgacure 2959 and Irgacure 819 for printing micron-scaled gradients of rigidity in polyacrylamide; The surface density of the adhesive cues on micron-scaled rigidity patterns; Mixed cell culture on a fibronectin-coated "concentric" hydrogel in the NBs culture medium; Confinement by rigidity gradients of other cell types; Glial cell organization on rigidity patterns of different widths; Partial dehydration of the surface of the gel causes nonuniform surface functionalization (PDF)

■ AUTHOR INFORMATION

Corresponding Authors

Caterina Tomba − *Univ. Grenoble Alps, CNRS, LTM and CNRS, Grenoble INP, Institut Néel, 38000 Grenoble, France;* Present Address: Univ Lyon, CNRS, INSA Lyon, Ecole Centrale de Lyon, Université Claude Bernard Lyon 1, CPE Lyon, INL, UMR5270, 69622 Villeurbanne, France. (C.T.); orcid.org/0000-0003-4634-1073; Email: caterina.tomba@univ-lyon1.fr

Alice Nicolas − *Univ. Grenoble Alps, CNRS, LTM, 38000 Grenoble, France;* orcid.org/0000-0003-1758-1174; Email: alice.nicolas@cea.fr

Authors

Camille Migdal − *Univ. Grenoble Alps, CNRS, LTM, CEA, CNRS, Inserm, BIG-BCI, and CEA, Inserm, BIG-BGE, 38000 Grenoble, France;* Present Address: Cell&Soft, 17 av des Martyrs, 38000 Grenoble, France. (C.M.)

David Fuard − *Univ. Grenoble Alps, CNRS, LTM, 38000 Grenoble, France*

Catherine Villard − *Univ. Grenoble Alps, CNRS, Grenoble INP, Institut Néel, 38000 Grenoble, France;* Present Address: Univ. de Paris, CNRS, LIED, UMR 8236, 75013 Paris, France. (C.V.)

Complete contact information is available at: https://pubs.acs.org/10.1021/acsabm.1c01295

Notes

The authors declare the following competing financial interest(s): C.M. is founder and CEO of Cell&Soft, which sells stiffness-patterned hydrogels for 2D cell culture. A.N. is co-founder, shareholder, and scientific adviser of the company.

https://doi.org/10.1021/acsabm.1c01295
ACS Appl. Bio Mater. XXXX, XXX, XXX−XXX

■ ACKNOWLEDGMENTS

C.T. and C.V. are grateful to A. Triller and S. Colasse for graciously receiving us at the IBENS (Paris) and transmitting their expertise in primary brain cell culture. C.T. was funded by French Ministry of Research. C.M. acknowledges the support by CEA TechnoSanté program. C.T., C.V., and A.N. are indebted to D. Gulino-Debrac for providing animal facilities. This work was supported by ANR (ANR-12-JSVE5-0008).

■ REFERENCES

(1) Janmey, P. A.; McCulloch, C. A. Cell Mechanics: Integrating Cell Responses to Mechanical Stimuli. *Annu. Rev. Biomed. Eng.* **2007**, *9*, 1−34.
(2) Sun, Y.; Yong, K. M. A.; Villa-Diaz, L. G.; Zhang, X.; Chen, W.; Philson, R.; Weng, S.; Xu, H.; Krebsbach, P. H.; Fu, J. Hippo/YAP-mediated rigidity-dependent motor neuron differentiation of human pluripotent stem cells. *Nat. Mater.* **2014**, *13*, 599−604.
(3) Yeung, T.; Georges, P. C.; Flanagan, L. A.; Marg, B.; Ortiz, M.; Funaki, M.; Zahir, N.; Ming, W.; Weaver, V.; Janmey, P. A. Effects of substrate stiffness on cell morphology, cytoskeletal structure, and adhesion. *Cell Motil. Cytoskeleton* **2005**, *60*, 24−34.
(4) Engler, A. J.; Sen, S.; Sweeney, H. L.; Discher, D. E. Matrix elasticity directs stem cell lineage specification. *Cell* **2006**, *126*, 677−689.
(5) Wells, R. G. The role of matrix stiffness in regulating cell behavior. *Hepatology* **2008**, *47*, 1394−1400.
(6) Wolf, K.; Alexander, S.; Schacht, V.; Coussens, L. M.; von Andrian, U. H.; van Rheenen, J.; Deryugina, E.; Friedl, P. Collagen-based cell migration models in vitro and in vivo. *Semin. Cell Dev. Biol.* **2009**, *20*, 931−941.
(7) Sieminski, A. L.; Hebbel, R. P.; Gooch, K. J. The relative magnitudes of endothelial force generation and matrix stiffness modulate capillary morphogenesis in vitro. *Exp. Cell Res.* **2004**, *297*, 574−584.
(8) Wei, S. C.; Fattet, L.; Tsai, J. H.; Guo, Y.; Pai, V. H.; Majeski, H. E.; Chen, A. C.; Sah, R. L.; Taylor, S. S.; Engler, A. J.; Yang, J. Matrix stiffness drives epithelial-mesenchymal transition and tumour metastasis through a TWIST1-G3BP2 mechanotransduction pathway. *Nat. Cell Biol.* **2015**, *17*, 678−688.
(9) Fernández-Sánchez, M. E.; Barbier, S.; Whitehead, J.; Béalle, G.; Michel, A.; Latorre-Ossa, H.; Rey, C.; Fouassier, L.; Claperon, A.; Brullé, L.; Girard, E.; Servant, N.; Rio-Frio, T.; Marie, H.; Lesieur, S.; Housset, C.; Gennisson, J.-L.; Tanter, M.; Ménager, C.; Fre, S.; Robine, S.; Farge, E. Mechanical induction of the tumorigenic β-catenin pathway by tumour growth pressure. *Nature* **2015**, *523*, 92−95.
(10) Balgude, A. P.; Yu, X.; Szymanski, A.; Bellamkonda, R. V. Agarose gel stiffness determines rate of DRG neurite extension in 3D cultures. *Biomaterials* **2001**, *22*, 1077−1084.
(11) Georges, P. C.; Miller, W. J.; Meaney, D. F.; Sawyer, E. S.; Janmey, P. A. Matrices with compliance comparable to that of brain tissue select neuronal over glial growth in mixed cortical cultures. *Biophys. J.* **2006**, *90*, 3012−3018.
(12) Franze, K.; Gerdelmann, J.; Weick, M.; Betz, T.; Pawlizak, S.; Lakadamyali, M.; Bayer, J.; Rillich, K.; Gögler, M.; Lu, Y.-B.; Reichenbach, A.; Janmey, P.; Käs, J. Neurite branch retraction is caused by a threshold-dependent mechanical impact. *Biophys. J.* **2009**, *97*, 1883−1890.
(13) Jiang, F. X.; Yurke, B.; Schloss, R. S.; Firestein, B. L.; Langrana, N. A. Effect of dynamic stiffness of the substrates on neurite outgrowth by using a DNA-crosslinked hydrogel. *Tissue Eng. Part A* **2010**, *16*, 1873−1889.
(14) Kostic, A.; Sap, J.; Sheetz, M. P. RPTPalpha is required for rigidity-dependent inhibition of extension and differentiation of hippocampal neurons. *J. Cell Sci.* **2007**, *120*, 3895−3904.
(15) Koch, D.; Rosoff, W. J.; Jiang, J.; Geller, H. M.; Urbach, J. S. Strength in the periphery: growth cone biomechanics and substrate rigidity response in peripheral and central nervous system neurons. *Biophys. J.* **2012**, *102*, 452−460.
(16) Sur, S.; Newcomb, C. J.; Webber, M. J.; Stupp, S. I. Tuning supramolecular mechanics to guide neuron development. *Biomaterials* **2013**, *34*, 4749−4757.
(17) Chen, W.-H.; Cheng, S.-J.; Tzen, J. T. C.; Cheng, C.-M.; Lin, Y.-W. Probing relevant molecules in modulating the neurite outgrowth of hippocampal neurons on substrates of different stiffness. *PLoS One* **2013**, *8*, No. e83394.
(18) Chan, C. E.; Odde, D. J. Traction dynamics of filopodia on compliant substrates. *Science* **2008**, *322*, 1687−1691.
(19) Betz, T.; Koch, D.; Lu, Y.-B.; Franze, K.; Käs, J. A. Growth cones as soft and weak force generators. *Proc. Natl. Acad. Sci. U.S.A.* **2011**, *108*, 13420−13425.
(20) Tanaka, A.; Fujii, Y.; Kasai, N.; Okajima, T.; Nakashima, H. Regulation of neuritogenesis in hippocampal neurons using stiffness of extracellular microenvironment. *PLoS One* **2018**, *13*, No. e0191928.
(21) Koser, D. E.; Thompson, A. J.; Foster, S. K.; Dwivedy, A.; Pillai, E. K.; Sheridan, G. K.; Svoboda, H.; Viana, M.; Costa, L. d. F.; Guck, J.; Holt, C. E.; Franze, K. Mechanosensing is critical for axon growth in the developing brain. *Nat. Neurosci.* **2016**, *19*, 1592−1598.
(22) McIlvain, G.; Schwarb, H.; Cohen, N. J.; Telzer, E. H.; Johnson, C. L. Mechanical properties of the in vivo adolescent human brain. *Dev. Cogn. Neurosci.* **2018**, *34*, 27−33.
(23) Magistretti, P. J. Neuron-glia metabolic coupling and plasticity. *Exp. Physiol.* **2011**, *96*, 407−410.
(24) Molofsky, A. V.; Krenick, R.; Ullian, E.; Tsai, H.-h.; Deneen, B.; Richardson, W. D.; Barres, B. A.; Rowitch, D. H. Astrocytes and disease: a neurodevelopmental perspective. *Genes Dev.* **2012**, *26*, 891−907.
(25) Minev, I. R.; Moshayedi, P.; Fawcett, J. W.; Lacour, S. P. Interaction of glia with a compliant, microstructured silicone surface. *Acta Biomater* **2013**, *9*, 6936−6942.
(26) Moshayedi, P.; Ng, G.; Kwok, J. C. F.; Yeo, G. S. H.; Bryant, C. E.; Fawcett, J. W.; Franze, K.; Guck, J. The relationship between glial cell mechanosensitivity and foreign body reactions in the central nervous system. *Biomaterials* **2014**, *35*, 3919−3925.
(27) Wang, L.; Cossette, S. M.; Rarick, K. R.; Gershan, J.; Dwinell, M. B.; Harder, D. R.; Ramchandran, R. Astrocytes directly influence tumor cell invasion and metastasis in vivo. *PloS one* **2013**, *8*, No. e80933.
(28) Tomba, C.; Villard, C. Brain cells and neuronal networks: Encounters with controlled microenvironments. *Microelectron. Eng.* **2015**, *132*, 176−191.
(29) Provenzano, P. P. Tug of War at the Cell-Matrix Interface. *Biophys. J.* **2017**, *112*, 1739−1741.
(30) Moshayedi, P.; da F. Costa, L.; Christ, A.; Lacour, S.; Fawcett, J.; Guck, J.; Franze, K. Mechanosensitivity of astrocytes on optimized polyacrylamide gels analyzed by quantitative morphometry. *J. Phys.: Cond. Mater.* **2010**, *22*, 194114.
(31) Ciasca, G.; Sassun, T. E.; Minelli, E.; Antonelli, M.; Papi, M.; Santoro, A.; Giangaspero, F.; Delfini, R.; De Spirito, M. Nano-mechanical signature of brain tumours. *Nanoscale* **2016**, *8*, 19629−19643.
(32) Johnson, C. L.; McGarry, M. D. J.; Gharibans, A. A.; Weaver, J. B.; Paulsen, K. D.; Wang, H.; Olivero, W. C.; Sutton, B. P.; Georgiadis, J. G. Local mechanical properties of white matter structures in the human brain. *Neuroimage* **2013**, *79*, 145−152.
(33) Bouchonville, N.; Meyer, M.; Gaude, C.; Gay, E.; Ratel, D.; Nicolas, A. AFM mapping of the elastic properties of brain tissue reveals kPa/μm gradients of rigidity. *Soft Matter* **2016**, *12*, 6232−6239.
(34) Paiva, S.; Joanne, P.; Migdal, C.; Soler, E. L.; Hovhannisyan, Y.; Nicolas, A.; Agbulut, O. Polyacrylamide hydrogels with rigidity-independent surface chemistry show limited long-term maintenance of pluripotency of human induced pluripotent stem cells on soft substrates. *ACS Biomater. Sci. Eng.* **2020**, *6*, 340−351.

https://doi.org/10.1021/acsabm.1c01295
ACS Appl. Bio Mater. XXXX, XXX, XXX−XXX

(35) Sheth, S.; Jain, E.; Karadaghy, A.; Syed, S.; Stevenson, H.; Zustiak, S. P. UV Dose Governs UV-Polymerized Polyacrylamide Hydrogel Modulus. *Int. J. Polym.Sci.* **2017**, *2017*, 1−9.
(36) Meier, J.; Meunier-Durmort, C.; Forest, C.; Triller, A.; Vannier, C. Formation of glycine receptor clusters and their accumulation at synapses. *J. Cell Sci.* **2000**, *113*, 2783−2795.
(37) Zuidema, J. M.; Hyzinski-García, M. C.; Van Vlasselaer, K.; Zaccor, N. W.; Plopper, G. E.; Mongin, A. A.; Gilbert, R. J. Enhanced GLT-1 mediated glutamate uptake and migration of primary astrocytes directed by fibronectin-coated electrospun poly-L-lactic acid fibers. *Biomaterials* **2014**, *35*, 1439−1449.
(38) Qian, X.; Shen, Q.; Goderie, S. K.; He, W.; Capela, A.; Davis, A. A.; Temple, S. Timing of CNS cell generation: a programmed sequence of neuron and glial cell production from isolated murine cortical stem cells. *Neuron* **2000**, *28*, 69−80.
(39) Purschke, M.; Rubio, N.; Held, K. D.; Redmond, R. W. Phototoxicity of Hoechst 33342 in time-lapse fluorescence microscopy. *Photochem. Photobiol. Sci.* **2010**, *9*, 1634−1639.
(40) Tse, J. R.; Engler, A. J. Preparation of hydrogel substrates with tunable mechanical properties. *Curr. Protoc. Cell Biol.* **2010**, *47*, 10.16.1.
(41) Moeendarbary, E.; Weber, I. P.; Sheridan, G. K.; Koser, D. E.; Soleman, S.; Haenzi, B.; Bradbury, E. J.; Fawcett, J.; Franze, K. The soft mechanical signature of glial scars in the central nervous system. *Nat. Commun.* **2017**, *8*, 14787.
(42) Hiscox, L. V.; Johnson, C. L.; McGarry, M. D. J.; Perrins, M.; Littlejohn, A.; van Beek, E. J. R.; Roberts, N.; Starr, J. M. High-resolution magnetic resonance elastography reveals differences in subcortical gray matter viscoelasticity between young and healthy older adults. *Neurobiol. Aging* **2018**, *65*, 158−167.
(43) Meyer, M.; Bouchonville, N.; Gaude, C.; Gay, E.; Ratel, D.; Nicolas, A. The Micro-Mechanical Signature of Pituitary Adenomas: New Perspectives for the Diagnosis and Surgery. *Adv. NanoBiomed. Res.* **2021**, *1*, 2000085.
(44) Schregel, K.; Wuerfel née Tysiak, E.; Garteiser, P.; Gemeinhardt, I.; Prozorovski, T.; Aktas, O.; Merz, H.; Petersen, D.; Wuerfel, J.; Sinkus, R. Demyelination reduces brain parenchymal stiffness quantified in vivo by magnetic resonance elastography. *Proc. Natl. Acad. Sci. U.S.A.* **2012**, *109*, 6650−6655.
(45) Rosso, G.; Liashkovich, I.; Gess, B.; Young, P.; Kun, A.; Shahin, V. Unravelling crucial biomechanical resilience of myelinated peripheral nerve fibres provided by the Schwann cell basal lamina and PMP22. *Sci. Rep.* **2015**, *4*, 7286.
(46) Ong, W.; Marinval, N.; Lin, J.; Nai, M. H.; Chong, Y.-S.; Pinese, C.; Sajikumar, S.; Lim, C. T.; Ffrench-Constant, C.; Bechler, M. E.; Chew, S. Y. Biomimicking Fiber Platform with Tunable Stiffness to Study Mechanotransduction Reveals Stiffness Enhances Oligodendrocyte Differentiation but Impedes Myelination through YAP-Dependent Regulation. *Small* **2020**, *16*, No. e2003656.
(47) Lau, L. W.; Cua, R.; Keough, M. B.; Haylock-Jacobs, S.; Yong, V. W. Pathophysiology of the brain extracellular matrix: a new target for remyelination. *Nat. Rev. Neurosci.* **2013**, *14*, 722−729.
(48) Dertinger, S. K.; Jiang, X.; Li, Z.; Murthy, V. N.; Whitesides, G. M. Gradients of substrate-bound laminin orient axonal specification of neurons. *Proc. Natl. Acad. Sci. U.S.A.* **2002**, *99*, 12542−12547.
(49) Rosso, G.; Young, P.; Shahin, V. Mechanosensitivity of embryonic neurites promotes their directional extension and Schwann cells progenitors migration. *Cell. Physiol. Biochem.* **2017**, *44*, 1263−1270.
(50) Stabenfeldt, S. E.; LaPlaca, M. C. Variations in rigidity and ligand density influence neuronal response in methylcellulose-laminin hydrogels. *Acta Biomater* **2011**, *7*, 4102−4108.
(51) Jiang, S.; Cao, Z. Ultralow-Fouling, Functionalizable, and Hydrolyzable Zwitterionic Materials and Their Derivatives for Biological Applications. *Adv. Mater.* **2010**, *22*, 920−932.
(52) Sundararaghavan, H. G.; Monteiro, G. A.; Firestein, B. L.; Shreiber, D. I. Neurite growth in 3D collagen gels with gradients of mechanical properties. *Biotechnol. Bioeng.* **2009**, *102*, 632−643.
(53) Burute, M.; Jansen, K. I.; Mihajlovic, M.; Vermonden, T.; Kapitein, L. Matrix elasticity gradients guide neuronal polarity by controlling microtubule network mobility. *bioRxiv*, 2021.
(54) Wilson, C. L.; Hayward, S. L.; Kidambi, S. Astrogliosis in a dish: substrate stiffness induces astrogliosis in primary rat astrocytes. *RSC Adv.* **2016**, *6*, 34447−34457.
(55) Mih, J. D.; Sharif, A. S.; Liu, F.; Marinkovic, A.; Symer, M. M.; Tschumperlin, D. J. A multiwell platform for studying stiffness-dependent cell biology. *PLoS One* **2011**, *6*, No. e19929.
(56) Kandow, C. E.; Georges, P. C.; Janmey, P. A.; Beningo, K. A. Polyacrylamide Hydrogels for Cell Mechanics: Steps Toward Optimization and Alternative Uses. *Cell Mechanics* **2007**, *83*, 29−46.
(57) Evingür, G. A.; Aktaş, D. K.; Pekcan, Ö. In situ steady state fluorescence (SSF) technique to study drying of PAAm hydrogels made of various cross-linker contents. *Chem. Eng. Process. Process Intensif.* **2009**, *48*, 600−605.
(58) Tanaka, J.; Toku, K.; Zhang, B.; Ishihara, K.; Sakanaka, M.; Maeda, N. Astrocytes prevent neuronal death induced by reactive oxygen and nitrogen species. *Glia* **1999**, *28*, 85−96.
(59) Carnegie, J. A.; Cabaca, O. Extracellular matrix composition and resilience: two parameters that influence the in vitro migration and morphology of rat inner cell mass-derived cells. *Biol. Reprod.* **1993**, *48*, 287−299.
(60) Barnabé-Heider, F.; Wasylnka, J. A.; Fernandes, K. J. L.; Porsche, C.; Sendtner, M.; Kaplan, D. R.; Miller, F. D. Evidence that embryonic neurons regulate the onset of cortical gliogenesis via cardiotrophin-1. *Neuron* **2005**, *48*, 253−265.
(61) Moonen, G.; Rogister, B.; Leprince, P.; Rigo, J.-M.; Delré, P.; Lefebvre, P. P.; Schoenen, J. Chapter 6 Neurono-glial interactions and neural plasticity. *The Developing Brain* **1990**, *86*, 63−73.
(62) Hu, Y.; Huang, G.; Tian, J.; Qiu, J.; Jia, Y.; Feng, D.; Wei, Z.; Li, S.; Xu, F. Matrix stiffness changes affect astrocyte phenotype in an in vitro injury model. *NPG Asia Mater.* **2021**, *13*, 35.
(63) Vianay, B.; Senger, F.; Alamos, S.; Anjur-Dietrich, M.; Bearce, E.; Cheeseman, B.; Lee, L.; Théry, M. Variation in traction forces during cell cycle progression. *Biol. Cell* **2018**, *110*, 91−96.
(64) Barczyk, M.; Carracedo, S.; Gullberg, D. Integrins. *Cell Tissue Res.* **2010**, *339*, 269−280.
(65) Chen, L.; Vicente-Manzanares, M.; Potvin-Trottier, L.; Wiseman, P. W.; Horwitz, A. R. The integrin-ligand interaction regulates adhesion and migration through a molecular clutch. *PLoS One* **2012**, *7*, No. e40202.
(66) Fujiwara, H.; Gu, J.; Sekiguchi, K. Rac regulates integrin-mediated endothelial cell adhesion and migration on laminin-8. *Exp. Cell. Res.* **2004**, *292*, 67−77.
(67) Faia-Torres, A. B.; Goren, T.; Ihalainen, T. O.; Guimond-Lischer, S.; Charnley, M.; Rottmar, M.; Maniura-Weber, K.; Spencer, N. D.; Reis, R. L.; Textor, M.; Neves, N. M. Regulation of human mesenchymal stem cell osteogenesis by specific surface density of fibronectin: a gradient study. *ACS Appl. Mater. Interfaces* **2015**, *7*, 2367−2375.
(68) Bangasser, B. L.; Rosenfeld, S. S.; Odde, D. J. Determinants of maximal force transmission in a motor-clutch model of cell traction in a compliant microenvironment. *Biophys. J.* **2013**, *105*, 581−592.
(69) Stanton, A. E.; Tong, X.; Yang, F. Extracellular matrix type modulates mechanotransduction of stem cells. *Acta Biomater* **2019**, *96*, 310−320.
(70) Dupont, S.; Morsut, L.; Aragona, M.; Enzo, E.; Giulitti, S.; Cordenonsi, M.; Zanconato, F.; Le Digabel, J.; Forcato, M.; Bicciato, S.; Elvassore, N.; Piccolo, S. Role of YAP/TAZ in mechanotransduction. *Nature* **2011**, *474*, 179−183.

https://doi.org/10.1021/acsabm.1c01295
ACS Appl. Bio Mater. XXXX, XXX, XXX−XXX